

**METHODS & TECHNIQUES**

# Simultaneous high-resolution pH and spectrophotometric recordings of oxygen binding in blood microvolumes

Michael Oellermann, Hans-O. Pörtner and Felix C. Mark\*

**ABSTRACT**

Oxygen equilibrium curves have been widely used to understand oxygen transport in numerous organisms. A major challenge has been to monitor oxygen binding characteristics and concomitant pH changes as they occur *in vivo*, in limited sample volumes. Here we report a technique allowing highly resolved and simultaneous monitoring of pH and blood pigment saturation in minute blood volumes. We equipped a gas diffusion chamber with a broad-range fibre-optic spectrophotometer and a micro-pH optode and recorded changes of pigment oxygenation along oxygen partial pressure ( $P_{O_2}$ ) and pH gradients to test the setup. Oxygen binding parameters derived from measurements in only 15  $\mu$ l of haemolymph from the cephalopod *Octopus vulgaris* showed low instrumental error (0.93%) and good agreement with published data. Broad-range spectra, each resolving 2048 data points, provided detailed insight into the complex absorbance characteristics of diverse blood types. After consideration of photobleaching and intrinsic fluorescence, pH optodes yielded accurate recordings and resolved a sigmoidal shift of 0.03 pH units in response to changing  $P_{O_2}$  from 0 to 21 kPa. Highly resolved continuous recordings along pH gradients conformed to stepwise measurements at low rates of pH changes. In this study we showed that a diffusion chamber upgraded with a broad-range spectrophotometer and an optical pH sensor accurately characterizes oxygen binding with minimal sample consumption and manipulation. We conclude that the modified diffusion chamber is highly suitable for experimental biologists who demand high flexibility, detailed insight into oxygen binding as well as experimental and biological accuracy combined in a single setup.

**KEY WORDS:** Diffusion chamber, Oxygen equilibrium curve, Hemocyanin, Haemocyanin, Haemoglobin, pH optode, Octopus, Amphipod, Antarctic fish

**INTRODUCTION**

Since the first oxygen binding experiments by Paul Bert (Bert, 1878) and Carl Gustav von Hüfner (Hüfner, 1890) and the pioneering work by Bohr, Hasselbalch and Krogh (Bohr et al., 1904) dating back more than a century, oxygen binding experiments have served to understand human blood physiology and diseases (e.g. Chanutin and Curnish, 1967; Festa and Asakura, 1979) or the environmental adaptation of various organisms (e.g. Brix, 1983; Herbert et al., 2006; Meir et al., 2009; Scott, 2011), and have even resolved crime (Olson et al., 2010). Ever since, researchers have developed and refined techniques to comprehend the complex physiology of oxygen transport, leading to a variety of currently employed methods (supplementary material Table S1).

Alfred Wegener Institute for Polar and Marine Research, 27570 Bremerhaven, Germany.

\*Author for correspondence (FMark@awi.de)

Received 18 June 2013; Accepted 9 January 2014

Such analysis commonly involves the determination of oxygen affinity ( $P_{50}$ ). Accurate determination of  $P_{50}$  requires the control or monitoring of extrinsic factors such as temperature, carbon dioxide and particularly pH. Assessing the effects of pH and the variation of pH during transition from the oxygenated to the deoxygenated state, due to the oxygenation-dependent release or uptake of protons by the pigment (Haldane effect), requires knowledge of pH at different levels of saturation for the analysis of oxygen equilibrium curves (OECs). Conventionally, experimenters control pH by added buffers [e.g. Tris, HEPES (Brix et al., 1994)] or determine pH from sub-samples or separately conditioned samples (e.g. Seibel et al., 1999; Weber et al., 2008) and rarely directly in the original sample (Pörtner, 1990; Zielinski et al., 2001). While added buffers prevent pH changes and may help to address specific functional characteristics of the pigment [e.g. effects of inorganic ions (Mangum and Lykkeboe, 1979)], they disturb the fine tuning of oxygen binding (Brix et al., 1994) and block pH changes relevant as part of the oxygen transport process, which need to be included for a comprehensive picture of oxygen transport *in vivo*. A major challenge in monitoring pH has been the relatively large sample volume required to immerse a pH electrode and its reference electrode. Particularly, analysis in highly limited sample volumes or devices that employ thin blood films (e.g. diffusion chamber, HemOscan, Pwee 50; supplementary material Table S1) suffer from this constraint.

Further, while many commercially available devices have been designed for mammalian (including human) blood analysis (e.g. CO-Oximeter, HEMOX-Analyser), only few provide the flexibility needed for the analysis of non-model organism blood, characterized by small sample volumes, unusual spectra, extreme *in vitro* temperatures or high pH sensitivity.

Here we report a major step forward in the respective methodology, allowing the simultaneous analyses of pH and pigment absorbance in microvolumes of blood. The challenges successfully met by our technique comprise: (1) the parallel measurement of oxygenation, paired with the simultaneous monitoring of pH depending on oxygenation level; (2) the use of minimal sample volumes of 15  $\mu$ l; and (3) high-resolution recordings, facilitated by continuous recordings of broad-range spectra and pH.

We upgraded a gas diffusion chamber (Niesel and Thews, 1961; Sick and Gersonde, 1969; Sick and Gersonde, 1972; Bridges et al., 1984; Morris and Oliver, 1999; Weber et al., 2010) with an integrated fibre-optic micro-pH optode and a miniature broad-range fibre-optic spectrophotometer. The experimental setup offers high flexibility to produce accurate OECs and pH recordings from only minute volumes of sample.

**RESULTS AND DISCUSSION****Spectrophotometric measurements**

Using the modified diffusion chamber, we successfully performed measurements on haemolymph from *Octopus vulgaris* and

## List of symbols and abbreviations

$n_{50}$	Hill coefficient
OEC	oxygen equilibrium curve
$P_{50}$	oxygen affinity
$P_{CO_2}$	carbon dioxide partial pressure
$P_{O_2}$	oxygen partial pressure

*Eulimnogammarus verrucosus* and whole blood of *Pachycara brachycephalum* at various oxygen and carbon dioxide partial pressures ( $P_{O_2}$  and  $P_{CO_2}$ , respectively) and temperatures. The integrated broad-range spectrophotometer resolved 2048 data points per spectrum from 200 to 1100 nm and yielded characteristic absorbance spectra for haemolymph containing haemocyanin with an oxygenation-dependent peak at 347 nm (*O. vulgaris*; Fig. 1A), and multiple responsive peaks at 540, 575, 412 and 335 nm for oxygenated haemoglobin-bearing blood and at 553, 427 and 366 nm for deoxygenated haemoglobin-bearing blood (*P. brachycephalum*; Fig. 1B). In addition, to the haemocyanin peak at 336 nm, haemolymph from *E. verrucosus* showed absorbance features above 400 nm that explain its green coloration (Fig. 1C). The detailed broad-range spectra strongly facilitate and enhance the analysis of solutions with complex absorbance spectra. Studies that gather only snapshots of the spectrum by means of single wavelength filters (e.g. Morris et al., 1985; Rasmussen et al., 2009) limit their experimental setup to a particular pigment type and may miss further relevant features.

The modified diffusion chamber yielded reproducible and accurate results employing both conventional stepwise measurements along an oxygen partial pressure ( $P_{O_2}$ ) gradient (Fig. 2) as well as measurements along a pH gradient (Fig. 3), designed for pH-sensitive pigments such as cephalopod haemocyanins (Pörtner, 1990). OECs of *O. vulgaris* haemolymph constructed from five replicated experiments with discrete oxygenation steps at constant  $P_{CO_2}$  (1 kPa) showed low variability among OECs and the derived parameters (Fig. 2, Table 1; supplementary material Fig. S1), with a relative error of 0.93% for  $P_{50}$  and 2.74% for the Hill coefficient,  $n_{50}$ . This low instrumental error and the good agreement of  $P_{50}$  and  $n_{50}$  with published data on *O. vulgaris* haemolymph recorded at the same temperature and pH (Table 1, Fig. 4) underline the accuracy of the setup. The Bohr coefficient recorded at 15°C was higher than that reported in Brix et al. (Brix et al., 1989), but closely matched values reported for *O. vulgaris* by Houlihan et al. (Houlihan et al., 1982) and Bridges (Bridges, 1995) *Octopus dofleini* [-1.7; pH 7.0–8.3 (Miller, 1985)] or *Octopus*

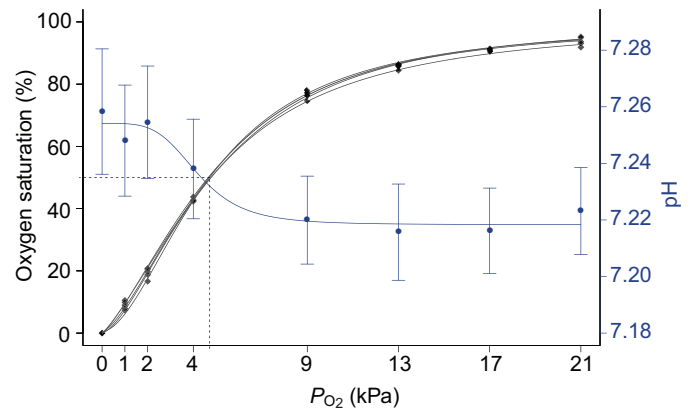


**Fig. 2. Replicated ( $n=5$ ) oxygen equilibrium curves of haemolymph from one *Octopus vulgaris* specimen obtained by stepwise changes to discrete  $P_{O_2}$  at constant  $P_{CO_2}$  (1 kPa).** Five parameter logistic curves were fitted and individually plotted for each measurement to illustrate instrumental variability. Haemolymph pH (means  $\pm$  s.e.m., blue), recorded by an optical pH microsensor immersed in the same sample droplet, changed sigmoidal and reverse directional to pigment saturation (black). The pH at half saturation (mean  $\pm$  s.e.m. =  $7.23 \pm 0.018$ ) can be derived from the intersection between  $P_{50}$  (dashed line) and the fitted pH line.

*macropus* [-1.99; pH 7.3–7.5 (Lykkeboe and Johansen, 1982)] (Fig. 4, Table 1). The difference in Bohr coefficients with those in the study by Brix et al. (Brix et al., 1989) relates to the pH ranges used to determine the Bohr coefficient. In octopods,  $P_{50}$  increases linearly with pH and levels off at lower pH ( $\sim 7.0$ ; Fig. 4) (Miller, 1985) as oxygen binding becomes pH insensitive (see 13 kPa OEC, Fig. 3). Brix et al. (Brix et al., 1989) included pH values below 7.0 (6.85–7.40), which consequently led to reduced regression slopes and underestimated Bohr coefficients. Thus, agreement with studies using pH ranges above 7.0 confirms the accuracy of Bohr coefficients determined with the modified diffusion chamber.

Both pigment absorbance and haemolymph pH responded to changes in gas composition within 30 s (Fig. 5). The recording of one OEC, including calibration at 100% and 0% oxygen saturation, lasted on average  $3.5 \pm 0.23$  h for measurements ( $n=5$ ) with eight discrete oxygenation steps and  $5.2 \pm 0.21$  h for measurements ( $n=4$ ) with eight discrete pH steps. While the maximum absorbance signal at 347 nm (haemocyanin oxygenation peak) drifted by  $-3.5 \pm 0.6\%$  per hour ( $n=5$ ), minimal absorbance remained nearly constant ( $0.27 \pm 0.21\%$ ,  $n=5$ ). The protein peak drifted less and varied more

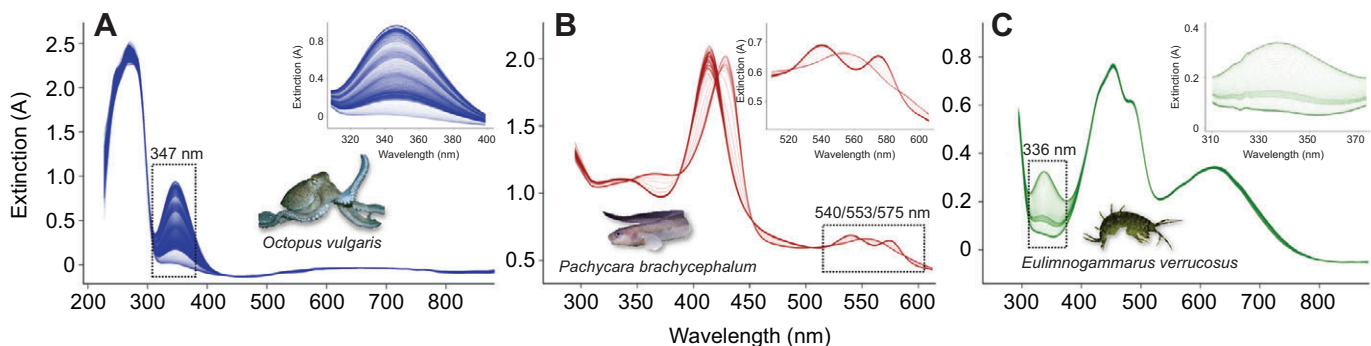


**Fig. 1. Highly resolved spectral changes of several non-model organisms.** (A) Broad-range spectra of haemolymph from *Octopus vulgaris* (15°C), measured at 4 kPa  $P_{O_2}$  from high to low pH (ca. 8.2–6.8). Exemplary, broad-range spectral recordings of whole blood from (B) the Antarctic eelpout *Pachycara brachycephalum* (0°C) and (C) of haemolymph from the Lake Baikal amphipod *Eulimnogammarus verrucosus* (6°C) reveal complex absorbance features. Spectral zones responding to oxygenation are marked by boxes and magnifications are shown in the insets. Spectra were coloured according to the visual appearance of the respective haemolymph/blood type. (Animal photos reprinted with permission by: Vladimir Motyčka, Christoph Held and Lena Jakob.)

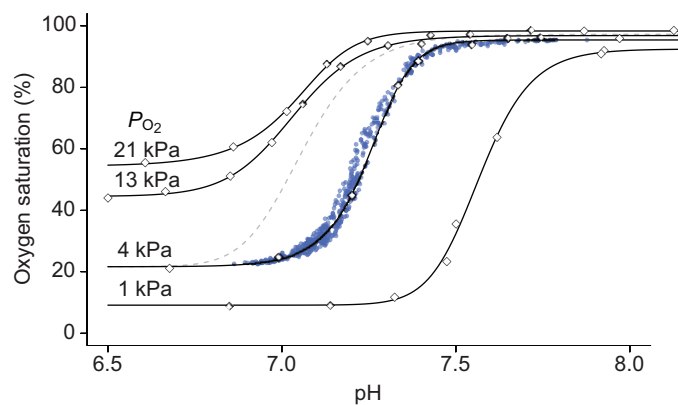


**Fig. 3.** Stepwise oxygen equilibrium curves (OECs) along a pH gradient (Pörtner, 1990), each derived from 15  $\mu$ l *Octopus vulgaris* haemolymph and measured by means of the modified diffusion chamber at 15°C and decreasing pH and various constant  $P_{O_2}$  (1, 4, 13 and 21 kPa). The continuous OEC recorded at slow rates of  $P_{CO_2}$  changes (0.015 kPa min<sup>-1</sup>, blue points) was highly resolved and closely matched the stepwise curves, while at faster rates the OEC shifted left (dashed grey curve).

among experiments ( $2.3 \pm 2.7\%$ ,  $n=5$ ; Fig. 5B). Negative drift observed for the maximum oxygenation signal was reported previously and explained by autoxidation of the blood pigment (Wells and Weber, 1989). Consequently, each measurement needs to comprise calibration steps with pure oxygen at the beginning and end to determine and include the apparent and constant drift in the calculation of pigment oxygenation by readjusting maximum absorbance at each consecutive oxygenation step (Wells and Weber, 1989). The less pronounced positive drift of the protein peak (Fig. 5B) indicates a low degree of sample drying and no apparent dilution by condensation or denaturation of the haemolymph sample.

Interestingly, the height of the protein peak did not remain stable, but increased/decreased upon oxygenation/deoxygenation (Fig. 5; supplementary material Fig. S2). This unexpected response of the protein peak to oxygenation/deoxygenation of the pigment (Fig. 5; supplementary material Fig. S2) cannot be ascribed to irreversible protein denaturation as the protein absorbance increased again upon re-oxygenation. Consequently, oxygenation status may affect protein absorbance spectra and thus measurements of protein concentration

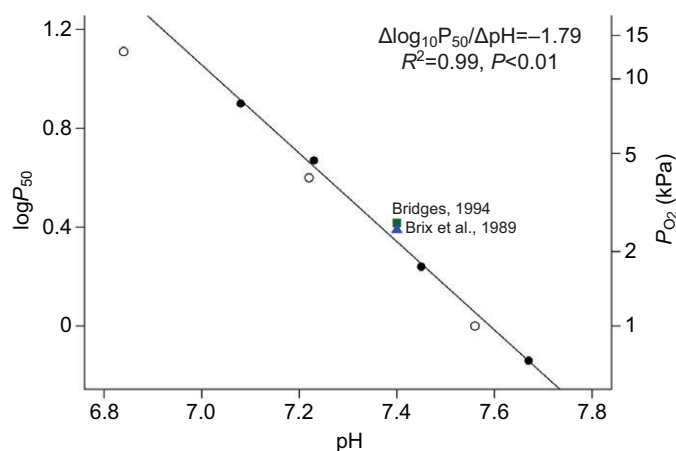


**Fig. 4.** Bohr plot illustrating the pH dependence of oxygen affinity ( $P_{50}$ ) of *Octopus vulgaris* haemolymph measured at 15°C.  $P_{50}$  from experiments with stepwise changes of  $P_{O_2}$  (filled circles) and pH (open circles) agreed with literature data [blue triangle (Brix et al. 1989); green square (Bridges, 1995)]. The data point at 13 kPa was excluded from the linear regression fit as  $P_{50}$  leveled off at low pH (~7.0).

in haemolymph or blood. Conformational changes depending on the degree of oxygenation may affect the absorbance features of the aromatic tryptophan, tyrosine and phenylalanine residues that account for the absorbance at 270–295 nm (Alexander and Ingram, 1980). Although the protein peak may not always vary with oxygen content (Bolton et al., 2009), it would be advisable to test a given blood type for such oxygenation dependency.

#### pH recordings in blood microvolumes

Simultaneous monitoring of pH, using a pH micro-optode in the same 15  $\mu$ l sample, yielded stable recordings within the calibrated range between pH 6.5 and 8.2. In response to changing  $P_{O_2}$  (0–21 kPa), these recordings were sufficiently precise to resolve a sigmoidal shift by 0.03 pH units, running in reverse to the OEC (Fig. 2). This shift denotes the oxygenation-dependent, lowered affinity of the pigment for protons (Haldane effect) and agrees well with other studies [e.g. *Carcinus maenas*  $\Delta$ pH=0.02 (Truchot, 1976)]. A sigmoidal rather than linear change of pH (Lapennas et al., 1981) may correspond to the linked sigmoidal trajectory of

**Table 1.** Comparison of blood physiological parameters of *Octopus vulgaris* haemolymph with literature data

Source	$P_{50}$ (kPa)	$n_{50}$	Bohr coefficient	pH	Temperature (°C)	
Present study	0.72	1.56	<b>-1.79</b> (pH 7.1–7.7)	7.68	15	
	1.72	1.59		7.45		
	4.72 (0.07)	1.75 (0.07)		7.23 (0.046)		
	7.94	1.61		7.08		
	<b>2.20<sup>a</sup></b>	–		7.4		
Brix et al., 1989	<b>2.45</b>	1.5	<b>-1.34</b> (pH 6.85–7.4)	7.4	15	
	4.41	1.6		-1.10 (pH 6.85–7.4)	7.4	25
	3.20	2.6 <sup>b</sup>		<b>-1.58/-1.73</b> (pH 7.2–7.6/7.3–7.7)	7.588	22
4.09	2.9 <sup>b</sup>	7.520				
4.80	3.5 <sup>b</sup>	7.415				
6.76	2.9 <sup>b</sup>	7.327				
Bridges, 1995	1.91	–	-1.86	7.4	10	
	<b>2.61</b>	–	<b>-1.83</b>	7.4	15	

$P_{50}$ , oxygen affinity;  $n_{50}$  Hill coefficient. Bold values denote parameters recorded under the same conditions. Values in parentheses for  $P_{50}$ ,  $n_{50}$  and pH represent  $\pm 95\%$  confidence intervals.

<sup>a</sup> $P_{50}$  extrapolated from linear regression line of Bohr plot at pH 7.4 (Fig. 4).

<sup>b</sup>Hill coefficients were recalculated from Houlihan et al. (Houlihan et al., 1982).

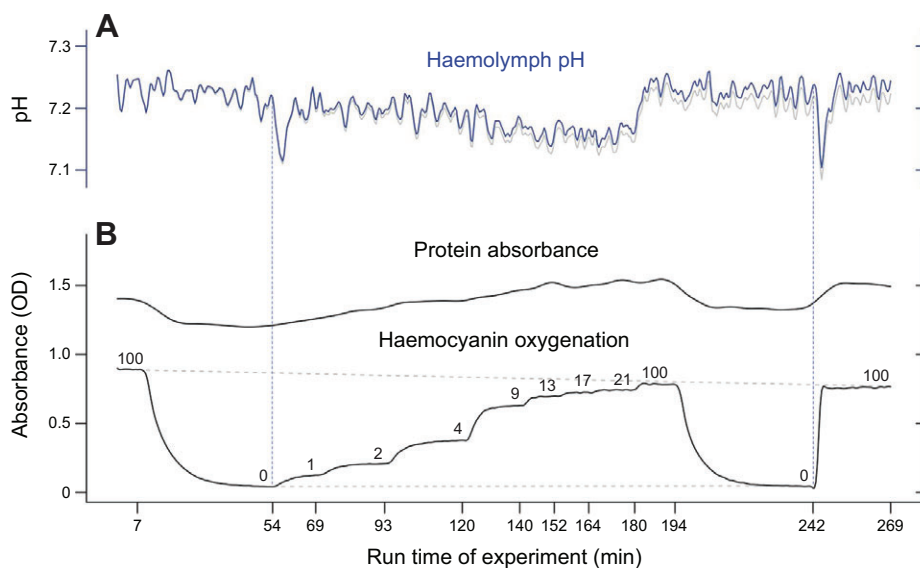


**Fig. 5. Change of haemolymph pH and wavelength-specific absorbance during an oxygen equilibrium measurement.** Response of (A) pH (uncorrected, grey trace; corrected by instrumental pH drift, blue trace) and (B) absorbance of the oxygenation-dependent peak (347 nm) and the protein peak of *Octopus vulgaris* haemolymph to stepwise changes of  $P_{O_2}$  recorded at 15°C. Numbers above the absorbance trace indicate  $P_{O_2}$  (kPa) of each oxygenation step. Horizontal dashed lines indicate the change of maximal and minimum absorbance (at 347 nm) over time, and vertical dashed lines the sudden but reversible pH changes upon initial oxygenation.

oxygen binding. The continuous recording of pH further revealed pronounced but reversible decreases of  $\sim 0.1$  pH units upon initial oxygenation, which indicates a high affinity state for protons in fully deoxygenated haemocyanins (Fig. 5).

$P_{50}$  derived from OECs recorded along pH gradients matched those recorded along  $P_{O_2}$  gradients and together showed a linear interdependence of pH and  $P_{50}$  in the pH range between 7.1 and 7.7 (Fig. 4). The OEC recorded by a continuous decrease of pH was highly resolved ( $\sim 500$  data points; Fig. 6) and fully equilibrated at slow  $P_{CO_2}$  changes of  $0.015 \text{ kPa min}^{-1}$ , as confirmed by the close match with the stepwise OEC (Fig. 3). This further underlines the validity of this alternative methodology, designed for pH-sensitive pigments. Simultaneous pH recordings, as in the present study, allow construction of highly resolved, continuous OECs from which blood parameters may be directly derived without curve modelling (Fig. 3). At faster rates ( $0.045 \text{ kPa min}^{-1}$ ), the OEC shifted left as saturation required longer to stabilize than pH (Fig. 3). A shift of continuous OEC at higher rates of change of  $P_{CO_2}$  or  $P_{O_2}$  has been explained by dislike equilibration rates with the surrounding gas between the sensor and the sample, due to differences in their physical properties or their relative position [‘dynamic error’ (Lapennas et al., 1981)]. However, as the pH optode was immersed in the sample, gas diffusion rates between the sample and the sensor

were likely similar, suggesting some delay in oxygenation of octopus haemocyanin in response to pH changes.

The signal of the pH optode drifted by  $-0.016$  pH units per 100 recordings ( $\pm 0.004$ ) and was corrected accordingly (Fig. 5A). This drift was higher than stated by the manufacturer ( $-0.0035$  pH units per 100 recordings) (PreSens, 2004; PreSens, 2012), probably because of incomplete protection from the light beam of the UV-VIS light source and resulting photobleaching of the optode’s fluorescent dyes. Thus, pH optodes may be re-calibrated prior to each measurement and the pH signal corrected for instrumental signal drift. Light exposure and therefore pH signal drift can be reduced by a software-controlled shutter in the light path that opens only during measurements or by using optically isolated sensor tips. The pH signal was also corrected for autofluorescence emitted by the sample, which decreased the pH signal in haemolymph by 0.06 units. Optical isolation but also calibration in the analysed medium can reduce or prevent the effects by intrinsic fluorescence between 530 and 660 nm, caused by, for example, porphyrine structures, which affect phase and amplitude of the pH raw signal (PreSens, C. Krause, personal communication).

#### Advantages and disadvantages

The modified diffusion chamber benefits the analysis of oxygen binding in several ways. Simultaneous recording of pigment oxygenation and pH allows characterization of oxygen binding and intrinsic pH responses under conditions mimicking *in vivo* conditions. Minute sample volumes facilitate the analysis of blood from small organisms or less invasive and repeated sampling from the same individual. Small sample volumes reduce the need to pool blood, facilitate replicate measurements and shorten measurement time because of accelerated gas equilibration. Highly resolved broad-range spectra capture detailed spectral properties of the pigment and promote the analysis of diverse blood types. Thin optical microsensors (for pH or  $P_{O_2}$ ) deliver stable and rapid recordings down to  $0^\circ\text{C}$  (M.O., unpublished observation) and allow recording of continuous and highly resolved OECs (Fig. 3). The gain of detail improves the accuracy of biophysical oxygen binding models, particularly if OECs do not follow a simple sigmoidal shape (Wells and Weber, 1989). The additional flexibility to operate at a large range of experimental temperatures and gas compositions makes this device not only highly suitable for standard applications

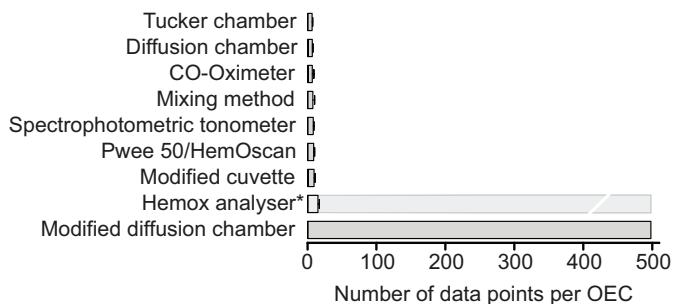


**Fig. 6. Number of data points (means  $\pm$  95% CI) for single oxygen equilibrium curves (OECs) compared between different methods (for references, see supplementary material Table S2).** The modified diffusion chamber method refers to continuous OEC measurements along a pH gradient. \*While some studies record fewer data points, recording intervals may be maximized to  $1 \text{ s}^{-1}$ .

but particularly for the functional analysis of blood from non-model organisms.

The use of optical microsensors and thin layers of blood also require specific care. The fluorescent dyes of the pH optodes are prone to photobleaching, which can be overcome by optical isolation or determination and correction for signal drift. Effects of intrinsic fluorescence of the sample are resolved by optical isolation, calibration in the same type of sample or by an initial cross-validation of pH with a pH electrode. The non-linear dynamic range of pH optodes restricts accurate recordings to pH values between 5.5 and 8.5, which, however, suffices in most of the blood-physiological experiments. Optical pH sensors that cover the extreme and even the full pH range may soon remove this limitation (Safavi and Bagheri, 2003). Further, the 150  $\mu\text{m}$  sensor tip breaks easily and requires careful handling. Like pH electrodes, pH optodes require calibration with buffers of similar ionic strength as the sample analysed and at the same experimental temperature (PreSens, 2004). Some blood types may clog on the sensor tip, which can be avoided by bathing the pH optode in a heparin solution (1000 units  $\text{ml}^{-1}$ ). Lastly, thin layers of blood are at higher risk of desiccation (Reeves, 1980), particularly at higher temperatures. Measures to avoid desiccation include decreased gas flow or covering of the blood sample with a gas permeable Teflon membrane (Reeves, 1980; Lapennas and Lutz, 1982; Clark et al., 2008).

### Conclusions

In this study we showed that a diffusion chamber upgraded with a broad-range spectrophotometer and a fibre-optical pH sensor allows for parallel measurement of pH and pigment saturation in microvolumes of blood samples. The setup yields reproducible and accurate results and offers high flexibility regarding the type of samples and experimental setting. The availability of optical  $P_{\text{O}_2}$  or  $P_{\text{CO}_2}$  probes and the rapid development of other optical sensor types (e.g. nitrogen oxide) suggest a broad array of future implementations that will help to address novel biological questions.

## MATERIALS AND METHODS

### Experimental setup and modifications

A gas diffusion chamber (Eschweiler Co., Kiel, Germany) designed and described in detail previously (Niesel and Thews, 1961; Sick and Gersonde, 1969; Sick and Gersonde, 1972) has been used to determine OECs by recording absorbance of a thin layer of a haemoglobin- or haemocyanin-bearing solution during continuous or stepwise changes of  $P_{\text{O}_2}$  (Wells and Weber, 1989). The original principle, characterized by full pigment deoxygenation with nitrogen gas followed by the time-dependent diffusion of oxygenated gas into the chamber (Niesel and Thews, 1961; Sick and Gersonde, 1969), was essentially abolished in subsequent studies that continuously perfused the chamber with defined gas mixtures (e.g. Bridges et al., 1984; Morris and Oliver, 1999; Weber et al., 2010). We adopted this amendment and further modified the diffusion chamber as follows. (1) A broad-range (200 to 1100 nm) fibre-optic spectrophotometer (USB2000+, Ocean Optics, USA) was connected via two fibre-optic cables fitted to the central cylinder of the diffusion chamber to direct the light beam via collimating lenses from the deuterium halogen light source (DT-Mini-2-GS, Ocean Optics) through the sample glass plate back to the 2048-element CCD-array detector of the spectrophotometer (Fig. 7; supplementary material Table S3). (2) The plastic slide that holds the sample glass plate in the light tunnel was modified to fit a fibre-optic micro-pH optode (NTH-HP5-L5-NS\*25/0.8-OIW, PreSens, Germany), housed in a syringe and connected to a phase detection device ( $\mu\text{PDD}$  3470, PreSens; Figs 7, 8). The needle of the syringe was then inserted through a silicone ring to prevent the leakage of gas (Fig. 8). In contrast to pH electrodes, pH optodes exhibit very small sensor tips (<150  $\mu\text{m}$ ) and determine pH from the intensity ratio between two pH-sensitive fluorescent dyes (PreSens, 2004). The modified diffusion chamber has been registered under patent number 10 2013 011 343 at the Deutsches Patent- und Markenamt, Germany.

The water reservoir of the diffusion chamber was filled with a 20% ethylene glycol solution (anti-freeze agent, AppliChem, Germany) and the temperature was monitored and controlled by means of a supplied temperature sensor (PreSens, Germany) and a connected circulating thermostatted water bath (LAUDA Ecoline Staredition RE 104, Germany). A gas mixing pump (Wösthoff, Germany) supplied an adjustable mixture of nitrogen, oxygen and carbon dioxide gas, humidified by an integrated scrubber to prevent desiccation of the sample (Fig. 8).

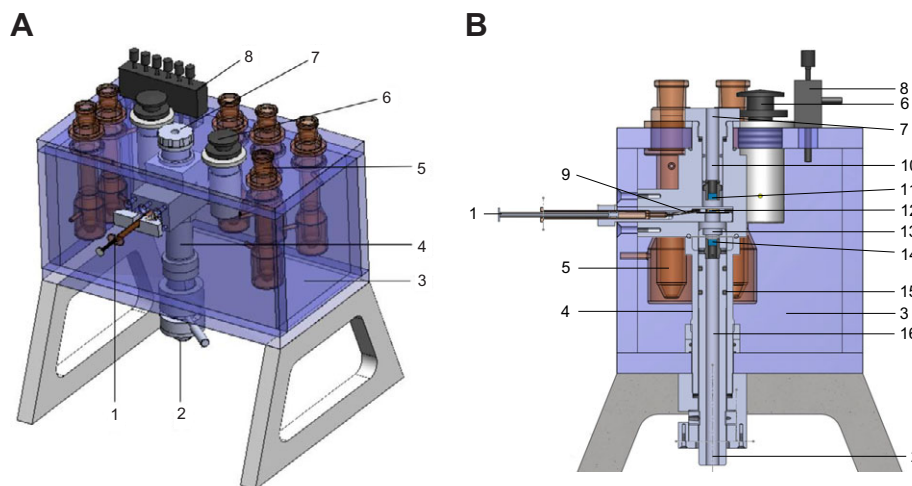


**Fig. 7. Illustration of the modified diffusion chamber.** (A) 3D model of the modified diffusion chamber and (B) a detailed cross-section through the central cylinder of the gas diffusion chamber illustrating the embedded fibre-optic micro-pH optode and an upper and lower custom-made tube containing collimating lenses and fittings for incoming and outgoing fibre-optic cables of the light source and the broad-range spectrophotometer. 1, Syringe housing for the pH micro optode; 2, fibre-optic cable exit to the spectrophotometer; 3, temperature-controlled water reservoir; 4, central cylinder containing optical devices; 5, gas-washing flask; 6, control wheel for gas distribution; 7, fibre-optic cable inlet from the light source; 8, control panel for gas inflow; 9, needle housing for the fibre-optic sensor tip; 10, upper custom-made tube, housing a collimating lens and the fibre-optic cable from the light source; 11, upper collimating lens; 12, blood sample spread on a glass plate; 13, spacer to keep 10 mm minimal distance between collimating lens and sample; 14, lower collimating lens; 15, rubber to seal lower tubing; 16, lower custom-made tube, housing a collimating lens and the fibre-optic cable leading to the spectrophotometer. Illustrations were drawn with 3D CAD software (SolidWorks, version 12.0; files available at <http://doi.pangaea.de/10.1594/PANGAEA.831205>).

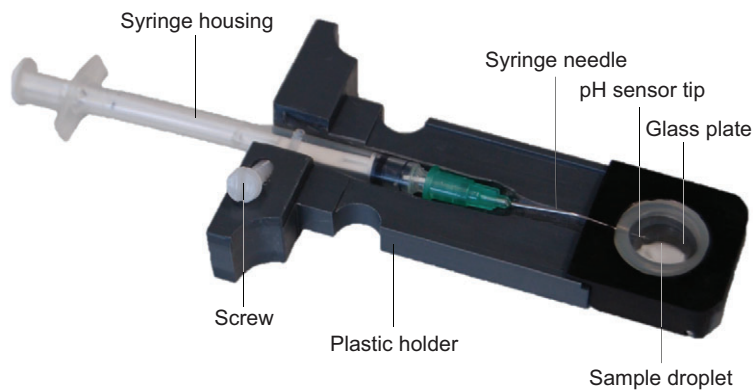


**Fig. 8.** Detailed illustration of the pH optode housed in a syringe, mounted with a screw and fitted to a plastic holder, which is moved into the gas-tight compartment centred in the diffusion chamber. The bended syringe needle is inserted through a silicon ring, which prevents gas leakage, and the sensor tip moved into the edge of the sample droplet located on a silica glass plate.

Prior to each experiment, we performed a six-point calibration (pH 6.7, 7.0, 7.2, 7.4, 7.7 and 8.1) of the pH optode, in MOPS-buffered [40 mmol l<sup>-1</sup>, 3-(*N*-morpholino)-propanesulfonic acid], filtered artificial seawater (35 PSU) at the corresponding experimental temperature. pH of buffers was checked with a pH glass electrode (InLab Routine Pt1100, Mettler Toledo, Germany) and a pH meter (pH 330i, WTW, Germany), calibrated with low ionic strength pH standards (AppliChem, Germany, DIN19266) and corrected to the free scale pH with Tris-buffered seawater standard (CO<sub>2</sub> QCLab, batch 4 2010, Dickson, USA) (Dickson, 2010) equilibrated at the same temperature. Aliquots of 18 µl of haemolymph (octopus or amphipod) were thawed on ice, shortly spun down to collect content (5 s at 1000 g), and 0.35 µl of 0.2 mmol l<sup>-1</sup> NaOH (4.6 µmol l<sup>-1</sup> final concentration) was added to raise haemolymph pH above 8.0 to ensure full pigment oxygenation. To avoid haemolysis and the formation of methaemoglobin by freezing, we used freshly sampled whole blood from *P. brachycephalum* and diluted the sample with one volume of blood plasma to improve light transmission during the measurement. The pH of haemolymph or whole blood was not stabilized with extrinsic buffers such as Tris or HEPES as they disturb the effects by ligands and temperature on pigment oxygenation (Brix et al., 1995). We then spread out 15 µl of haemolymph or whole blood on the glass plate without contacting the sealing ring. The pH optode needle was inserted through the sealing ring and the sensor tip moved into the edge of the droplet to reduce bleaching of the dye by the light beam passing through the centre of the glass plate (Fig. 8). Both the glass plate holder and the fitted pH optode were then inserted and fixed in the diffusion chamber (Fig. 7). The spectrophotometer required the recording of light and dark spectra without blood sample before each measurement and was set to 15 ms integration time, averaging 100 scans per recording and 30 s measurement intervals. pH drift of the pH optode was evaluated by measuring the pH difference of a MOPS-buffered seawater pH standard (pH 7.2) at 15°C before and after each experiment. Effects of intrinsic fluorescence were assessed by comparing pH recordings of the pH optode and the pH electrode in octopus haemolymph at 15°C.

Using *O. vulgaris* haemolymph, we tested the setup via two previously employed methodologies. OECs were obtained (1) by stepwise changes of discrete  $P_{O_2}$  (1, 2, 4, 9, 13, 17 and 21 kPa) at constant  $P_{CO_2}$  (e.g. Wells and Weber, 1989) or (2) by stepwise as well as continuous decreases of pH by means of increasing CO<sub>2</sub> concentrations (0–20 kPa) and constant  $P_{O_2}$  (e.g. Pörtner, 1990). While stepwise measurements allow the sample to fully equilibrate at several successive but discrete  $P_{O_2}$  or pH steps (Lapennas et al., 1981; Pörtner, 1990), continuous measurements characterize a constant change and monitoring of  $P_{O_2}$  or pH (Wells and Weber, 1989). Each experiment involved calibration with pure nitrogen as well as pure oxygen at the beginning and at the end to determine the drift of the maximum absorbance signal. The exemplary analysis of whole blood of *P. brachycephalum* was performed from 21 to 0 kPa  $P_{O_2}$  and pH 8.2–7.1 at 0°C and of thawed haemolymph of *E. verrucosus* at a constant  $P_{O_2}$  of 21 kPa and pH 7.7–6.9 at 6°C.

## Animals

One major incentive to advance this method was to enhance the investigation of non-model organisms, which often suffer from instrumental restrictions (e.g. sample volume, wavelength filters, temperature setting) by devices optimised for human or rodent blood. We thus chose three non-model organisms with diverse experimental demands to test the flexibility and

accuracy of the modified diffusion chamber. The cephalopod *Octopus vulgaris* Cuvier 1797 lives between 11 and 18°C and has evolved a closed circulatory system containing blue haemolymph with high concentrations [54.3±6.9 g l<sup>-1</sup> (Wells and Smith, 1987; Brix et al., 1989)] of the extracellular, pH-sensitive respiratory pigment haemocyanin, which evolved independently from arthropod haemocyanin (van Holde et al., 2001). Published data on *O. vulgaris* blood physiology allowed us to test the accuracy of the modified diffusion chamber. The Antarctic eelpout *Pachycara brachycephalum* (Pappenheim 1912) lives at freezing temperatures, yields only little blood and circulates intracellular haemoglobin at – for teleosts – low concentrations (37.4 g l<sup>-1</sup>) in a closed system. The Baikal amphipod *Eulimnogammarus verrucosus* (Gerstfeldt 1858) lives at 5–6°C and yields small amounts of green haemolymph that transports oxygen via extracellular haemocyanin (45.3±7.9 g l<sup>-1</sup>) in an open vascular system (Wirkner and Richter, 2013).

*Octopus vulgaris* specimens were hand-caught by snorkelling at Banuyls sur Mer, France, at 16°C. Animals were anaesthetized in 3% EtOH (Ikeda et al., 2009), and after withdrawing haemolymph from the cephalic vein, were finally killed by a cut through the brain following sampling. *Pachycara brachycephalum* was caught on the Polarstern cruise ANTXXV/4 near Maxwell Bay at King George Island, Antarctica, in May 2009 using fish traps, transported to the Alfred Wegener Institute, Bremerhaven, Germany, and kept in aerated tanks connected to a re-circulating aquaculture system at 0°C. The animal was anaesthetised with 0.3 g l<sup>-1</sup> tricaine methanesulphonate, blood was withdrawn using a heparinized syringe and the animal was finally killed by a spinal cut [animal research permit no. 522-27-11/02-00(93), Freie Hansestadt Bremen, Germany]. *Eulimnogammarus verrucosus* was collected in Bolshie Koty, Lake Baikal, Russia, during summer 2012, transported to Irkutsk, Russia, and kept in aerated 2.5 l tanks at 6°C. Haemolymph was withdrawn using a dorsally inserted capillary. All haemolymph samples were centrifuged at 15,000 g for 15 min at 0°C to remove cell debris and stored at –20°C.

## Data analysis

The processing, time-matching and analysis of data from both the spectrophotometer and the pH meter were performed using the R statistical language (R Development Core Team, 2013) (for R scripts, see <http://doi.pangaea.de/10.1594/PANGAEA.831205>).

An integrated five-parameter logistic model [Eqn 1; R ‘drc’ add-on package (Ritz and Streibig, 2005)] was applied to fit sigmoidal curves to stepwise OECs:

$$f[x, (b, c, d, e, f)] = c + \frac{(d - c)}{\left(1 + \exp\left\{b \left[\log\left(\frac{x}{e}\right)\right]\right\}\right)} \quad (1)$$

The parameters  $c$  and  $d$  denote the upper and lower asymptotes, respectively, and  $f$  the asymmetry of the curve. The parameters  $b$  and  $e$  correspond to the slope and inflection point, respectively, of a four-parameter logistic model if the parameter  $f$  equals 1. Note that this equation represents an empirical curve fit that does not describe the functional properties of the haemocyanin sub-units according to mechanistic insight.

Oxygen affinity ( $P_{50}$ ) was interpolated from fitted OECs at half saturation and cooperativity (Hill’s coefficient,  $n_{50}$ ) was determined via Hill plots by regressing  $\log_{10}[Y/(1-Y)]$  versus  $\log_{10}P_{O_2}$  in the linear mid-range (~20–80%

saturation), with  $Y$  denoting the fractional saturation. The Bohr coefficient was calculated from the regression slope ( $\Delta \log_{10} P_{50}$  versus  $\Delta \text{pH}$ ) between pH 7.1 and 7.7. In pH/saturation diagrams,  $P_{50}$  denotes the  $\log_{10}$  of the oxygen isobar and the pH of the isobar at half saturation [pH<sub>50</sub> (Pörtner, 1990)]. Data were expressed as means  $\pm$  95% confidence intervals if not stated otherwise.

#### Acknowledgements

We thank Dr Jan Strugnell (La Trobe University, Bundoora) for providing lab space and her extensive support; Michael Imsic and all other staff and technicians of the La Trobe University for their kind support during the initial tests of the modified diffusion chamber; Erich Dunker, Matthias Littmann and Dirk Wethje (scientific workshop, Alfred Wegener Institute, Bremerhaven) for the technical modifications and drawings of the diffusion chamber; Lena Jakob for providing haemolymph samples from *Eulimnogammarus verrucosus*; Marian Y Hu for his help catching *Octopus vulgaris*; the logistics department of the Alfred Wegener Institute; and last of all Saumya Pant and little Yuva Lalit Pant for their enriching company. We further thank Roy Weber for his kind advice and the two anonymous reviewers for their many helpful remarks and suggestions on an earlier version of this manuscript. We dedicate this article to the memory of Steve Morris and express our special thanks to Maria Morris and Elizabeth Morgan (University of Bristol), who saved and donated the diffusion chamber to our department.

#### Competing interests

The authors declare no competing financial interests.

#### Author contributions

M.O. and F.C.M. conceived and developed the technical modifications, compiled the manuscript and interpreted results. M.O. performed the experiments and analysis. H.-O.P. initiated the discussion and contributed to data interpretation and manuscript editing.

#### Funding

This study was supported by a *Journal of Experimental Biology* travelling fellowship, a PhD scholarship by the German Academic Exchange Service (DAAD, D/11/43882) to M.O., the Deutsche Forschungsgemeinschaft (MA4271/1-2 to F.C.M.) and the Alfred Wegener Institute for Polar and Marine Research.

#### Supplementary material

Supplementary material available online at  
<http://jeb.biologists.org/lookup/suppl/doi:10.1242/jeb.092726/-/DC1>

#### References

- Alexander, J. B. and Ingram, G. A. (1980). A comparison of five of the methods commonly used to measure protein concentrations in fish sera. *J. Fish Biol.* **16**, 115-122.
- Bert, P. (1878). *La Pression Barométrique: Recherches de Physiologie Expérimentale*. Paris: G. Masson.
- Bohr, C., Hasselbalch, K. and Krogh, A. (1904). Über einen in biologischer Beziehung wichtigen Einfluss, den die Kohlensäurespannung des Blutes auf dessen Sauerstoffbindung übt. *Skand. Arch. Physiol.* **16**, 402-412.
- Bolton, J. C., Collins, S., Smith, R., Perkins, B., Bushway, R., Bayer, R. and Vetelino, J. (2009). Spectroscopic analysis of hemolymph from the American lobster (*Homarus americanus*). *J. Shellfish Res.* **28**, 905-912.
- Bridges, C. R. (1995). Bohr and root effects in cephalopod haemocyanins – paradox or pressure in *Sepia officinalis*? *Mar. Freshw. Behav. Physiol.* **25**, 121-130.
- Bridges, C. R., Morris, S. and Grieshaber, M. K. (1984). Modulation of haemocyanin oxygen affinity in the intertidal prawn *Palaemon elegans* (Rathke). *Respir. Physiol.* **57**, 189-200.
- Brix, O. (1983). Giant squids may die when exposed to warm water currents. *Nature* **303**, 422-423.
- Brix, O., Bårdgard, A., Cau, A., Colosimo, A., Condo, S. and Giardina, B. (1989). Oxygen-binding properties of cephalopod blood with special reference to environmental temperatures and ecological distribution. *J. Exp. Zool.* **252**, 34-42.
- Brix, O., Colosimo, A. and Giardina, B. (1995). Temperature dependence of oxygen binding to cephalopod haemocyanins: ecological implications. *Mar. Freshw. Behav. Physiol.* **25**, 149-162.
- Chanutin, A. and Curnish, R. R. (1967). Effect of organic and inorganic phosphates on the oxygen equilibrium of human erythrocytes. *Arch. Biochem. Biophys.* **121**, 96-102.
- Clark, T. D., Seymour, R. S., Wells, R. M. G. and Frappell, P. B. (2008). Thermal effects on the blood respiratory properties of southern bluefin tuna, *Thunnus maccoyii*. *Comp. Biochem. Physiol.* **150A**, 239-246.
- Dickson, A. (2010). The carbon dioxide system in seawater: equilibrium chemistry and measurements. In *Guide to Best Practices for Ocean Acidification Research and Data Reporting* (ed. U. Riebesell, V. J. Fabry, L. Hansson and J.-P. Gattuso). Luxembourg: Publications Office of the European Union.
- Festa, R. S. and Asakura, T. (1979). Oxygen dissociation curves in children with anemia and malignant disease. *Am. J. Hematol.* **7**, 233-244.
- Herbert, N. A., Skov, P. V., Wells, R. M. G. and Steffensen, J. F. (2006). Whole blood-oxygen binding properties of four cold-temperate marine fishes: blood affinity is independent of pH-dependent binding, routine swimming performance, and environmental hypoxia. *Physiol. Biochem. Zool.* **79**, 909-918.
- Houlihan, D., Innes, A., Wells, M. and Wells, J. (1982). Oxygen consumption and blood gases of *Octopus vulgaris* in hypoxic conditions. *J. Comp. Physiol. B* **148**, 35-40.
- Hüfner, G. (1890). Über das gesetz der dissociation des oxyhaemoglobins und über einige daran sich knüpfende wichtige fragen aus der biologie. *Arch. Anat. Physiol.* **1**, 1-27.
- Ikeda, Y., Sugimoto, C., Yonamine, H. and Oshima, Y. (2009). Method of ethanol anaesthesia and individual marking for oval squid (*Sepioteuthis lessoniana* Férussac, 1831 in Lesson 1830-1831). *Aquac. Res.* **41**, 157-160.
- Lapennas, G. N. and Lutz, P. L. (1982). Oxygen affinity of sea turtle blood. *Respir. Physiol.* **48**, 59-74.
- Lapennas, G. N., Colacino, J. M. and Bonaventura, J. (1981). Thin-layer methods for determination of oxygen binding curves of hemoglobin solutions and blood. In *Methods in Enzymology*, Vol. 76 (ed. E. Chianconi, L. Rossi-Bernardi and E. Antonini), pp. 449-470. London: Academic Press.
- Lykkeboe, G. and Johansen, K. (1982). A cephalopod approach to rethinking about the importance of the bohr and haldane effects. *Pac. Sci.* **36**, 305-313.
- Mangum, C. P. and Lykkeboe, G. (1979). The influence of inorganic ions and pH on oxygenation properties of the blood in the gastropod mollusc *Busycon canaliculatum*. *J. Exp. Zool.* **207**, 417-430.
- Meir, J. U., Champagne, C. D., Costa, D. P., Williams, C. L. and Ponganis, P. J. (2009). Extreme hypoxemic tolerance and blood oxygen depletion in diving elephant seals. *Am. J. Physiol.* **297**, R927-R939.
- Miller, K. I. (1985). Oxygen equilibria of *Octopus dofleini* hemocyanin. *Biochemistry* **24**, 4582-4586.
- Morris, S. and Oliver, S. (1999). Respiratory gas transport, haemocyanin function and acid-base balance in *Jasus edwardsii* during emersion and chilling: simulation studies of commercial shipping methods. *Comp. Biochem. Physiol.* **122A**, 309-321.
- Morris, S., Taylor, A. C., Bridges, C. R. and Grieshaber, M. K. (1985). Respiratory properties of the haemolymph of the intertidal prawn *Palaemon elegans* (Rathke). *J. Exp. Zool.* **233**, 175-186.
- Niesel, W. and Thews, G. (1961). Ein neues verfahren zur schnellen und genauen aufnahme der sauerstoffbindungskurve des blutes und konzentrierter hämoproteidlösungen. *Pflugers Arch.* **273**, 380-395.
- Olson, K. N., Hillyer, M. A., Kloss, J. S., Geiselhart, R. J. and Apple, F. S. (2010). Accident or arson: is CO-oximetry reliable for carboxyhemoglobin measurement postmortem? *Clin. Chem.* **56**, 515-519.
- Pörtner, H. O. (1990). An analysis of the effects of pH on oxygen binding by squid (*Illex illecebrosus*, *Loligo pealei*) haemocyanin. *J. Exp. Biol.* **150**, 407-424.
- PreSens (2004). *Instruction Manual pH-4 mini*. Regensburg, Germany: Precision Sensing GmbH.
- PreSens (2012). *Product Sheet for pH Microsensors*. Regensburg, Germany: Precision Sensing GmbH.
- R Development Core Team (2013). *R: A Language and Environment for Statistical Computing*. Vienna, Austria: R Foundation for Statistical Computing.
- Rasmussen, J. R., Wells, R. M. G., Henty, K., Clark, T. D. and Brittain, T. (2009). Characterization of the hemoglobins of the Australian lungfish *Neoceratodus forsteri* (Kreffl). *Comp. Biochem. Physiol.* **152A**, 162-167.
- Reeves, R. B. (1980). A rapid micro method for obtaining oxygen equilibrium curves on whole blood. *Respir. Physiol.* **42**, 299-315.
- Ritz, C. and Streibig, J. C. (2005). Bioassay analysis using R. *J. Stat. Softw.* **12**, 1-22.
- Safavi, A. and Bagheri, M. (2003). Novel optical pH sensor for high and low pH values. *Sens. Actuators B Chem.* **90**, 143-150.
- Scott, G. R. (2011). Elevated performance: the unique physiology of birds that fly at high altitudes. *J. Exp. Biol.* **214**, 2455-2462.
- Seibel, B., Chausson, F., Lallier, F., Zal, F. and Childress, J. (1999). Vampire blood: respiratory physiology of the vampire squid (Cephalopoda: Vampyromorpha) in relation to the oxygen minimum layer. *Exp. Biol. Online* **4**, 1-10.
- Sick, H. and Gersonde, K. (1969). Method for continuous registration of O<sub>2</sub>-binding curves of hemoproteins by means of a diffusion chamber. *Anal. Biochem.* **32**, 362-376.
- Sick, H. and Gersonde, K. (1972). Theory and application of the diffusion technique for measurement and analysis of O<sub>2</sub>-binding properties of very autoxidizable hemoproteins. *Anal. Biochem.* **47**, 46-56.
- Truchot, J. P. (1976). Carbon dioxide combining properties of the blood of the shore crab, *Carcinus maenas* (L.): CO<sub>2</sub>-dissociation curves and Haldane effect. *J. Comp. Physiol.* **112**, 283-293.
- van Holde, K. E., Miller, K. I. and Decker, H. (2001). Hemocyanins and invertebrate evolution. *J. Biol. Chem.* **276**, 15563-15566.
- Weber, R. E., Behrens, J. W., Malte, H. and Fago, A. (2008). Thermodynamics of oxygenation-linked proton and lactate binding govern the temperature sensitivity of O<sub>2</sub> binding in crustacean (*Carcinus maenas*) hemocyanin. *J. Exp. Biol.* **211**, 1057-1062.
- Weber, R. E., Campbell, K. L., Fago, A., Malte, H. and Jensen, F. B. (2010). ATP-induced temperature independence of hemoglobin-O<sub>2</sub> affinity in heterothermic billfish. *J. Exp. Biol.* **213**, 1579-1585.
- Wells, M. and Smith, P. (1987). The performance of the octopus circulatory system: a triumph of engineering over design. *Experientia* **43**, 487-499.
- Wells, R. M. G. and Weber, R. E. (1989). The measurement of oxygen affinity in blood and haemoglobin solutions. In *Techniques in Comparative Respiratory Physiology: An Experimental Approach* (ed. C. R. Bridges and P. J. Butler), pp. 279-303. Cambridge: Cambridge University Press.
- Wirkner, C. S. and Richter, S. (2013). Circulatory system and respiration. *The Natural History of the Crustacea* **1**, 376-412.
- Zielinski, S., Sartoris, F. J. and Pörtner, H. O. (2001). Temperature effects on hemocyanin oxygen binding in an antarctic cephalopod. *Biol. Bull.* **200**, 67-76.